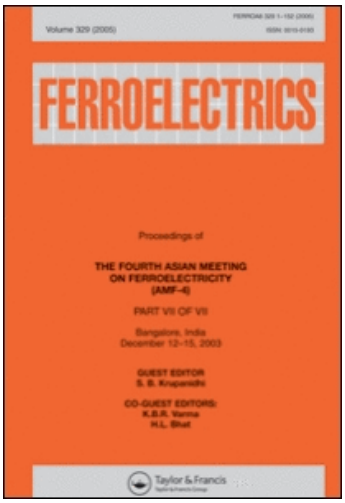

Ferroelectrics
Publication details, including instructions for authors and subscription information:
http://www.informaworld.com/smpp/title~content=t713617887

Predicted Performance of Ferroelectric Memory Capacitors under Mechanical Constraint

I. Pane [a]; N. A. Fleck [b]; D. P. Chu [bc]; J. E. Huber [d]
[a] Department of Civil Engineering, Bandung Institute of Technology, Bandung, Indonesia [b] Department of Engineering, University of Cambridge, Trumpington Street, UK [c] Electrical Engineering Division, Cambridge University, Cambridge, UK [d] Department of Engineering Science, University of Oxford, UK

Online Publication Date: 01 January 2008

To cite this Article Pane, I., Fleck, N. A., Chu, D. P. and Huber, J. E.(2008)'Predicted Performance of Ferroelectric Memory Capacitors under Mechanical Constraint',Ferroelectrics,370:1,219 — 225
To link to this Article: DOI: 10.1080/00150190802381704
URL: http://dx.doi.org/10.1080/00150190802381704

Ferroelectrics, 370:219–225, 2008

ISSN: 0015-0193 print / 1563-5112 online
DOI: 10.1080/00150190802381704

Taylor & Francis
Taylor & Francis Group

Predicted Performance of Ferroelectric Memory Capacitors under Mechanical Constraint

I. PANE,[1,*] N. A. FLECK,[2] D. P. CHU,[2,3] AND J. E. HUBER[4]

[1]Department of Civil Engineering, Bandung Institute of Technology, Ganesha 10, Bandung 40132, Indonesia
[2]Department of Engineering, University of Cambridge, Trumpington Street, CB4 1YE, UK
[3]Electrical Engineering Division, Cambridge University, 9 JJ Thompson Ave., Cambridge CB3 OFA, UK
[4]Department of Engineering Science, University of Oxford, Parks Road, OX1 3PJ, UK

The performance of one and two-dimensional ferroelectric memory capacitors characterized by the hysteresis of applied electric field versus the surface charge density is investigated using the finite element method. Sensitivity of the electrical hysteresis of the 2D capacitor constrained by compliant layers to selected geometrical variables is explored. The remnant polarization and the coercive filed are compared with those of a free-standing film and a film fully constrained by the substrate. The aspect ratio can significantly influence the clamping behavior and thus the remnant polarization of the capacitor.

Keywords Crystal plasticity; FeRAM; ferroelectric; polarization; thin film

1. Introduction

The market for non-volatile memory devices is growing. Among the leading candidates for such devices is the ferroelectric random access memory (FeRAM) capacitor. Its advantage includes fast read and write, highly re-writable, scalable, and compatible with current Si technology (Chu, 2004). This makes it a strong candidate for future memory devices in high speed computers. However, there remain some unresolved issues such as the main switching event activated during FeRAM operation and the small remnant polarization obtained for a thin film structure. If both 90° and 180° switching are active then the maximum remnant polarization can reach the saturation. However, 90° switching is strongly influenced by the mechanical field such as stress. Therefore, it is also sensitive to the state of mechanical constraint.

A typical FeRAM capacitor in a memory device obtained by TEM is shown Fig. 1. It comprises a ferroelectric layer sandwiched between two electrode layers and a very thin titanium layer below the lower electrode. The capacitor is encapsulated by a low dielectric material of SiO_2. This study is motivated by the fact that in such FeRAM capacitor the

Received September 3, 2007.
*Corresponding author. E-mail: ivpane@netscape.net

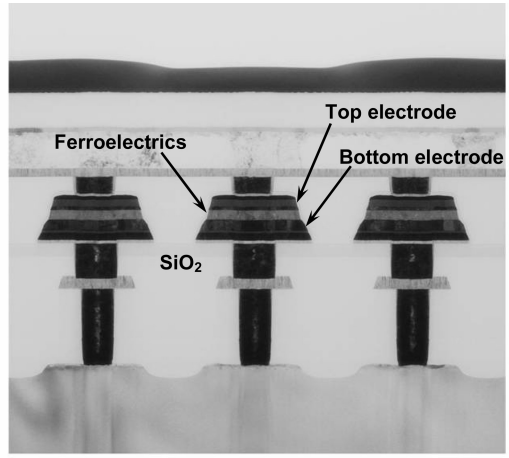

Figure 1. Cross-sectional TEM image of integrated ferroelectric thin film capacitors (with permission from Seiko-Epson, Japan).

ferroelectric layer is surrounded by solids that can constraint the stress-free transformation strain produced during 90° switching. With this kind of constraint 90° switching can be severely limited and the remnant polarization can fall far below the saturation. The main objectives of this study are to simulate the ferroelectric switching of a FeRAM capacitor under mechanical constraint and to predict its performance by analyzing the electrical hysteresis.

2. Theory and Models

2.1. Boundary Value Problem

An electromechanical boundary value problem of a solid geometry comprising of an elastic, ferroelectric material is considered. General Field equations and boundary conditions for the problem are described herein. The mechanical equilibrium demands $\sigma_{ij,j} = 0$, where σ_{ij} is the stress and the usual subscript notation is assumed. The small strain tensor relation $\varepsilon_{ij} = \frac{1}{2}(u_{i,j} + u_{j,i})$ is assumed. Unless otherwise stated, repeat suffices imply summations over the relevant dimensions, i.e. $i = 1, 2$ for the 2D case and $i = 1, 2, 3$ for the 3D case. The static electrical field in a ferroelectric body is dictated by Gauss's law relating the divergence of the electric displacement D_i to the free charge density q by $D_{i,i} - q = 0$. The electric field E_i is the negative gradient of the electric potential ϕ according to $E_i = -\phi_{,i}$. On the surface S of the body of unit outward normal n_i, the traction t_i balances the stressσ_{ij}, and the charge density Q balances the jump in the electric displacement D_i across S such that $t_i = n_i\sigma_{ij}$, $Q = n_i\,[D_i] = n_i(D_i^0 - D_i)$, where [] denotes the jump in a quantity across the boundary and D_i^0 denotes the electrical displacement exterior to the body.

2.2. Constitutive Law

The same rate dependent constitutive law proposed in Huber and Fleck, 2001 to model the single crystal ferroelectric behavior is used. The elastic strain is obtained by subtracting the remnant strain ε_{ij}^r, from the total strain ε_{ij}. Similarly, the reversible electric displacement

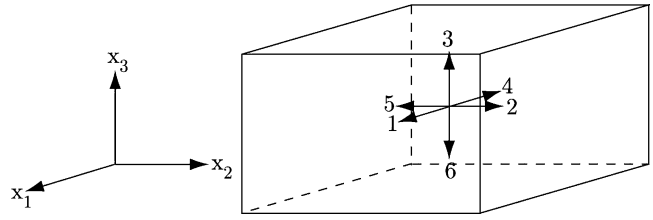

Figure 2. Domains in a [100]-oriented tetragonal crystal.

is obtained by subtracting the remnant polarization P_i from the total electric displacement D_i. The elastic strain and the reversible electric displacement follow the usual linear piezoelectric relations,

$$\sigma_{ij} = c_{ijkl}\left(\varepsilon_{kl} - \varepsilon^r_{kl}\right) - e_{kij}E_k \tag{1}$$

$$D_i = e_{ikl}\left(\varepsilon_{kl} - \varepsilon^r_{kl}\right) + \kappa^{\varepsilon}_{ik}E_k + P_i \tag{2}$$

where $e_{kij} = c_{ijmn}d_{kmn}$, $\kappa^{\varepsilon}_{ik} = \kappa^{\sigma}_{ik} - d_{irs}c_{pqrs}d_{kpq}$, κ^{σ}_{ik} is the dielectric permittivity tensor, c_{ijkl} is the elastic stiffness tensor, and d_{kij} is the piezoelectric tensor.

Domain switching is described by the crystal plasticity theory detailed in Huber et al., 1999 and Huber and Fleck, 2001. It will only be briefly described here. A single tetragonal crystal of ferroelectric with six variants or domains of polarization is considered (Fig. 2). The total number of the switching or transformation systems that can be simultaneously active is 15 and each system is denoted by the index α. It is assumed that the I^{th} domain has a transversely isotropic piezoelectric tensor:

$$d^I_{ijk} = d_{33}n_in_jn_k + d_{31}(n_i\delta_{jk} - n_in_jn_k) + d_{15}(\delta_{ij}n_k - 2n_in_jn_k + \delta_{ik}n_j) \tag{3}$$

as characterized by the three constants d_{33}, d_{31}, and d_{15}. The vector n_i indicates the polarization direction. Each domain has a volume fraction c_I and is subjected to the same macroscopic uniform stress σ_{ij} and electric field E_i. Both the linear and remnant parts of the strain ε_{ij} and of the electric displacement D_i within the ferroelectric solid are given by volume-averages over the crystal. Consequently, the macroscopic piezoelectric tensor of the crystal d_{ijk} equals to $\sum_{I=1}^{M} c_I d^I_{ijk}$, where $M = 6$ is the number of total domains. For simplicity, the elastic stiffness c_{ijkl} and dielectric permittivity κ^{σ}_{ik} of each domain are taken to be isotropic and uniform. Then, (1) and (2) can be rewritten as:

$$\sigma_{ij} = c_{ijkl}\left(\varepsilon_{kl} - \varepsilon^r_{kl}\right) - \sum_{I=1}^{M} c_I e^I_{kij}E_k \tag{4}$$

$$D_i = \sum_{I=1}^{M} c_I e^I_{ikl}\left(\varepsilon_{kl} - \varepsilon^r_{kl}\right) + \kappa^{\varepsilon}_{ik}E_k + P_i \tag{5}$$

It is emphasized that the isotropic elasticity tensor c_{ijkl} depends only upon the Young's modulus E and Poisson ratio ν, while the isotropic permittivity tensor scales with a single constant κ. The piezoelectric tensor e^I_{kij} is related to d^I_{ijk} via $e^I_{kij} = c_{ijmn}d^I_{kmn}$.

Full switching of the α^{th} transformation generates a change of remnant strain by $\Delta\varepsilon^{r,\alpha}_{ij}$, of remnant polarization by ΔP^{α}_i, and of the piezoelectric tensor by Δd^{α}_{ijk}. If the I^{th} domain has a polarization vector n_i, then its remnant strain is $\varepsilon^{r,I}_{ij} = \varepsilon_0(n_in_j - \delta_{ij})/2$ which gives

$\Delta\varepsilon_{ij}^{r,\alpha} = \varepsilon_{ij}^{r,I} - \varepsilon_{ij}^{r,J}$. For a tetragonal lattice with two identical lattice constants a and a larger lattice constant c, the lattice strain is $\varepsilon_0 = (c-a)/a$. The change in remnant polarization ΔP_i^α is equal to $s_i^\alpha P_0$, where s_i^α is a unit vector in the direction of the change in remnant polarization and P_0 is the maximum polarization. The change in piezoelectric tensor is given by $\Delta d_{ijk}^\alpha = d_{ijk}^I - d_{ijk}^J$. Using these quantities, the driving force for α^{th} transformation G^α is defined as:

$$G^\alpha = \sigma_{ij}\Delta\varepsilon_{ij}^{r,\alpha} + E_i\Delta P_i^\alpha + \sigma_{ij}\Delta d_{ijk}^\alpha E_k \tag{6}$$

The rate of change of domain volume fraction for the α^{th} transformation is denoted by a scalar $\dot{f}^\alpha$. It depends upon G^α normalized by the critical driving force G_c^α and upon the volume fraction involved in the α^{th} transformation, normalized by the initial fraction (c_0) according to:

$$\dot{f}^\alpha = \dot{f}_0 \left|\frac{G^\alpha}{G_c^\alpha}\right|^{m-1} \frac{G^\alpha}{G_c^\alpha} \left(\frac{c_I}{c_0}\right)^{1/k} \tag{7}$$

In the above, $\dot{f}_0$ plays the role of a reference rate of switching. The rate of change of remnant strain, remnant polarization, and of the piezoelectric tensor read:

$$\dot{\varepsilon}_{ij}^r = \sum_{\alpha=1}^{N} \dot{f}^\alpha \Delta\varepsilon_{ij}^{r,\alpha}, \quad \dot{P}_i = \sum_{\alpha=1}^{N} \dot{f}_0^\alpha \Delta P_i^\alpha, \quad \dot{d}_{ijk} = \sum_{\alpha=1}^{N} \dot{f}^\alpha \Delta d_{ijk}^\alpha \tag{8}$$

In the rate independent limit, G_c^α is the energy barrier for α^{th} transformation. Its value is determined by considering the one-dimensional case of a free-standing film under uniaxial electrical loading. Assume that the solid has six possible polarization directions as shown in Fig. 2, with unit normal to the film aligned in the x_3 direction. Relation (6) then gives $G_c^{180} = 2E_{180}P_0$ and $G_c^{90} = \sqrt{2}E_{90}P_0$, where E_{180} and E_{90} are the electric field required for 180° and 90° switching.

The initial conditions for any switching event include an initial stress state and the initial volume fraction of ferroelectric domains. In principle, these initial conditions can be found by evaluating the processing route taken to produce the FeRAM device. Here, we limit our scope to a film that is initially in the state of zero residual stress and contains an equal volume fraction of all domains.

2.3. Finite Element Model

The above constitutive law can be recast in a form suitable for finite element implementation. A standard displacement and electric potential-based FE formulation assuming plane strain condition has been chosen. In the case of a linear piezoelectric constitutive law, the formulation is similar to that of Alik and Hughes, 1970. The variational statement is written in rate form, and integrated step-by-step by the rate tangent method including an equilibrium correction term, to give

$$\begin{aligned} \Delta t \int_V [\dot{\sigma}_{ij}\delta\varepsilon_{ij} + \dot{D}_i\delta E_i]dV &= \Delta t \int_S [\dot{t}_i\delta u_i - \dot{Q}\delta\phi]dS \\ + \left\{ \int_S [t_i\delta u_i - Q\delta\phi]dS - \int_V [\sigma_{ij}\delta\varepsilon_{ij} + D_i\delta E_i]dV \right\} & \end{aligned} \tag{9}$$

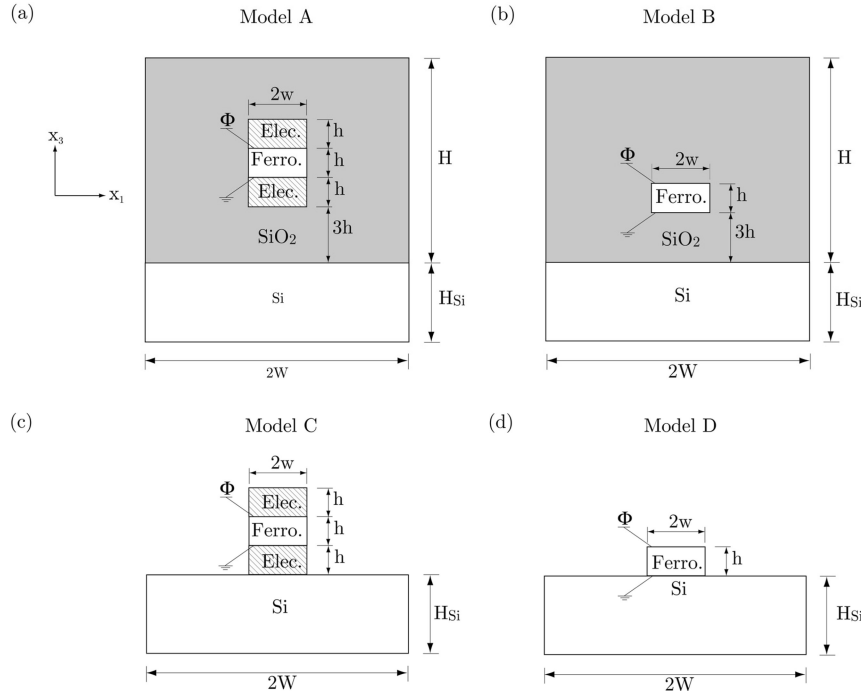

Figure 3. Structures and geometry of two dimensional models.

The last term in curly brackets ensures continued equilibrium. The rate tangent method is chosen to improve the numerical stability of the nonlinear problem. It has been frequently used in the context of the crystal plasticity modeling of metals (Peirce et al., 1983 and Needleman et al., 1985). The full derivation of the rate tangent method for solving the nonlinear ferroelectric problem and its implementation into the finite element method have been given in Pane et al.

A typical FeRAM capacitor shown in Fig. 1 is modeled according to Fig. 3. The plane strain direction is parallel to x_2. The complete model is A and the other models represent various states where the presence of some surrounding solids can be neglected. Models A and B include the passivation medium and models C and D do not. The latter models assume the electrode layers to be very thin such that their presences are neglected. The above modeling allows to study the relative contribution of individual constraining layer. For all 2D models, the ferroelectric island structure rests on a Si substrate, and the full geometry is meshed using a 6-node triangular element with H, H_{Si}, and W are sufficiently large: $H = 20$ h, $H_{Si} = 15$ h, $W = 10$ w. This choice is made in order to simulate the constraint imposed by a half space of SiO_2 passivation and a half space of Si substrate. Perfect bonding at interfaces between two materials are assumed. Furthermore, the capacitor is subjected to a cyclic voltage loading $\Phi(t)$ at the electrodes (parallel to x_3 axis) with a magnitude corresponding to about three times the coercive field ($3E_c$) and a frequency of $5000\dot{f}_0$ until the electrical hysteresis loop is stable. We limit our study to the following ferroelectric material parameters: $r = G_c^{90}/G_c^{180} = 1$, $E = 160$ GPa and $\nu = 0.3$, $P_0 = 0.5$, $\varepsilon_0 = 1\%$, $d_{33} = 300 \times 10^{-12}$ m/V, $d_{31} = -135 \times 10^{-12}$ m/V, $d_{15} = 525 \times 10^{-12}$ m/V, $\kappa = 5 \times 10^{-9}$, $m = 5$, $k = 1$, $\dot{f}_0 = 2\ \mathrm{s}^{-1}$, and $E_{180} = 2$ MV/m. The surrounding solids are fixed: Pt electrode

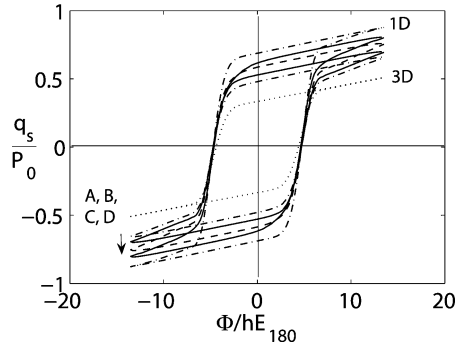

Figure 4. Hysteresis loops of an island obtained from models A, B, and D compared to that of the thin ferroelectric layer under 3D constraint, $\bar{w} = 0.5$ and $\bar{r} = 0.5$.

with $E = 160$ GPa and $\nu = 0.38$, SiO_2 passive layer with $E = 50$ GPa and $\nu = 0.2$, and Si substrate with $E = 160$ GPa and $\nu = 0.2$.

3. Performance of a Capacitor

The electrical hysteresis of the averaged surface charge density q_s versus the applied voltage $\Phi E_{180}/h$ obtained from each model can be seen in Fig. 4. Only the final stable loop is shown. We have observed that in the first cycle both 90° and 180° switching can take place but after the first cycle the main switching event only 180°. This happens since domains are aligned in the direction of the applied field during the first loading cycle. After this, the domains switch more easily by 180° event.

The role of constraint on performance will be analyzed for a two dimensional (2D) capacitor having $w/h = 1$. The performance will be evaluated in terms of remnant polarization which is the value of q_s when the applied voltage is zero. Higher remnant polarization means that the capacitor is more sensitive and can be read more accurately. First, it can be seen that the coercive field which is the value of applied field when $q_s = 0$ is not influenced by the type of constraint. Second, it is seen that removing the passivation layer can increase the remnant polarization. Further increase in remnant polarization is obtained when the thickness of electrode layers are made negligible compare to that of the ferroelectric layer. The relative contribution of each layer bonded to the ferroelectric layer follows exactly the same sequence as the model, meaning D is less constrained than C, B and A, and C is less constrained than B and A and so on. This also implies that in model contribution of 90° switching towards the remnant polarization is more dominant in model D compared to models C, B and A.

The result from the two dimensional (2D) models is also compared with that obtained from the simpler one dimensional model denoted by symbols 1D and 3D. In the one dimensional model the electrical and mechanical fields are considered uniform. Symbol 1D denotes that the ferroelectric film that is constrained only in the plane strain direction perpendicular to x_3 axis and to the direction of applied field. Symbol 3D denotes that the condition of zero strain in all principal directions is imposed. The performance of 2D models appears to be in between that of the two cases of one dimensional model. This shows how the performance of a 2D capacitor can be roughly approximated by the one dimensional model.

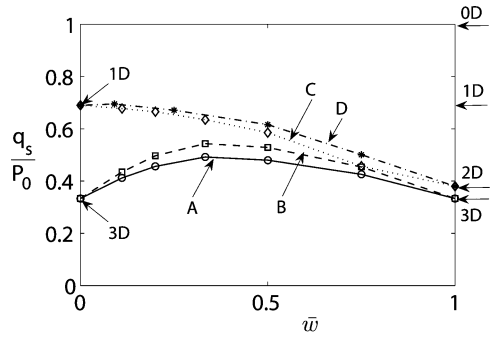

Figure 5. Variation of remnant charge density on top or bottom electrode with $\bar{w}$ obtained from models A, B, C, and D, $\bar{r} = 0.5$.

The aspect ratio $\bar{w} = w/(w + h)$, of a 2D capacitor plays an important role. There are two extreme limits: $\bar{w}$goes to zero corresponds to a thin sheet of ferroelectric standing on Si substrate and $\bar{w}$goes to one corresponds to a thin ferroelectric film bonded to Si substrate. The remnant polarization changes with$\bar{w}$according to Fig. 5. For models A and B, it is clear that the state of $\bar{w}$goes to zero is the same as that of $\bar{w}$goes to one, i.e. the state of zero strain or 3D constraint. However for models C and D, $\bar{w}$approaching zero means a state of 1D constraint (in plane strain direction alone). As a consequence the result predicts that there is a maximum remnant polarization for models A and B which occurs at $\bar{w}$around 0.3.

4. Concluding Remarks

The effect of geometry upon the performance of a FeRAM capacitor has been predicted. It is found that the presence of elastic layers bonded to the ferroelectric film can suppress the remnant polarization down to a state similar to a thin ferroelectric film without any strain allowed. The performance of a 2D FeRAM capacitor can be expected to be between that of a one dimensional thin film with 1D constraint and of a film with 3D constraint.

For a capacitor with a passivation layer, the performance can be maximized by choosing the right aspect ratio. If no passivation is presence then the performance can be improved by minimizing the aspect ratio.

References

Alik, H., Hughes, T. J. R. Finite element method for piezoelectric vibration. *Int. J. Numer. Meth. Eng.* **2**, 151–157 (1970).

Chu., D. P. Ferroelectric random access memory (FeRAMS) cells and non-destructive read-out (NDRO). Proceedings of 3rd ECS International Semiconductor Technology Conference (ISTC), 94–99 (2004).

Huber, J. E., Fleck, N. A., Landis, C. M., McMeeking, R. M. A constitutive model for ferroelectric polycrystals. *J. Mech. Phys. Solids*. **47** (8), 1663–1697 (1999).

Huber, J. E., Fleck, N. A. Multi-axial electrical switching of a ferroelectric: theory versus experiment. *J. Mech. Phys. Solids*. **49** (4), 785–811 (2001).

Needleman, A., Asaro, R. J., Lemonds, J., Peirce, D. Finite element analysis of crystalline solids. *Comp Methods App. Mech. Eng*. **52** (1–3), 689–708 (1985).

Pane, I., Fleck, N. A., Huber, J. E., Chu, D. P. Effect of geometry upon the performance of a thin film memory capacitor. Accepted for publication.

Peirce, D. Asaro, R. J., Needleman, A. Material rate dependence and localized deformation in crystalline solids. *Acta Met*. **31** (12), 1951–1976 (1983).